

## GRAIN TEMPERATURE AND INFRARED EMISSION FROM CARBON DUST OF MIXED COMPOSITION

S. BARTLETT

Department of Physics, University of Waterloo, Waterloo, Ontario, Canada N2L 3G1

AND

W. W. DULEY<sup>1</sup>

Department of Physics, University College, University of NSW, Australian Defence Force Academy, Canberra, ACT, Australia

Received 1995 August 3; accepted 1996 January 5

### ABSTRACT

The equilibrium temperature of carbonaceous dust grains whose composition is consistent with IR spectra of diffuse cloud and dense cloud dust has been calculated using random covalent network (RCN) solutions for amorphous dust having a mixed graphite, diamond, and polymeric hydrocarbon composition. An effective medium approximation has been adopted to describe optical and thermal constants for dust compositions consistent with IR absorption spectra. A small amount of  $sp^2$  hybridized carbon in the form of aromatic rings is found to have a significant effect in reducing equilibrium temperature in dust with high diamond/polymer content. This formalism has also been used to calculate nonequilibrium emission spectra of very small grains (VSGs) subjected to stochastic heating in the interstellar radiation field. Such grains are found to emit strongly in sharp IR bands associated with C-H bonds at  $3.4\ \mu\text{m}$  and longer wavelengths. The effect of varying graphite/diamond/hydrocarbon composition on nonequilibrium emission by VSGs can also be described using this formalism. The ratio of emission at 12 and  $25\ \mu\text{m}$  is found to be high for VSGs with a large fraction of diamond or polymeric hydrocarbon but decreases dramatically for dust with a large  $sp^2$  aromatic component.

*Subject headings:* dust, extinction — infrared: ISM: lines and bands

### 1. INTRODUCTION

Infrared absorption spectra of dust in a variety of interstellar environments indicate the presence of a carbonaceous solid whose composition is variable and contains a range of  $sp^2$  and  $sp^3$  hybridized bonded carbon species (Wickramasinghe & Allen 1980; Butchart et al. 1986; Adamson, Whittet, & Duley 1990; Sandford et al. 1991; Allamandola et al. 1992; Pendleton et al. 1994). Discrete absorption features attributable to  $\text{CH}_2$ ,  $\text{CH}_3$ , and tertiary CH have been observed. A detection of aromatic CH has also been reported (Sellgren, Smith, & Brooke 1994; Pendleton et al. 1994).

Such solids can be modeled as a random covalent network (RCN) (Duley 1995) using the formalism that has been applied to other amorphous solids (Angus & Jensen 1988; Jones 1990). For carbons, the RCN formalism has been shown to be useful in the prediction of a range of physical properties including optical band gap and IR absorption (Tamor & Wu 1990; Tamor, Vassell, & Carduner 1991; Angus & Hayman 1988). The RCN approach yields a quantitative estimate of the relative proportion of various  $sp^2$  and  $sp^3$  components such as aromatic, diamond-like, and aliphatic chemical groups in such solids. When applied to interstellar carbons (Duley 1995), RCN solutions provide compositions that are compatible with the relative strength of individual IR absorption features and the abundance of carbon contained in these solids. The evolution of the chemical composition and hydrogen content of carbonaceous dust in response to

environmental factors can also be traced using the constraints of a random covalent network. These requirements eliminate many possible chemical compositions that might be expected in the absence of topological and bonding constraints and permit one to associate a specific range of chemical compositions and grain structures with particular interstellar environments.

A fundamental parameter in obtaining further information concerning grain properties is the dust temperature  $T_d$  and specifically how  $T_d$  relates to the chemical composition of carbonaceous solids as inferred from IR spectra in which such solids are consistent with RCN solutions. In a previous study (Pinho & Duley 1994), the equilibrium temperature of carbonaceous dust grains with variable  $sp^2/sp^3$  composition has been calculated using an effective medium approximation. It was found that a change in the relative proportion of  $sp^2$  and  $sp^3$  bonded carbon can have a profound effect on  $T_d$ , particularly in solids with little aromatic  $sp^2$  bonded carbon. In this paper, we extend these calculations to include carbon dust compositions compatible with both RCN constraints and IR absorption in diffuse and dense cloud environments. We also calculate emission spectra for very small grains (VSGs) subject to thermal spiking and find that such grains can emit strongly in the  $\text{CH}_2$  and  $\text{CH}_3$  aliphatic resonances at  $\sim 3.4\ \mu\text{m}$ .

Our approach, then, is to use available IR data to constrain the range of carbon dust compositions according to the RCN formalism, and then to predict other properties of such dust. In the past, such properties have been calculated under the assumption that dust is either “graphite” or “amorphous carbon.” The present technique permits an exploration of the properties of other carbon solids that may be more representative of dust in interstellar clouds.

<sup>1</sup> Present address: Guelph-Waterloo Center for Graduate Work in Physics, Waterloo, Ontario, Canada N2L 3G1; wwduley@physics.watstar.uwaterloo.ca.

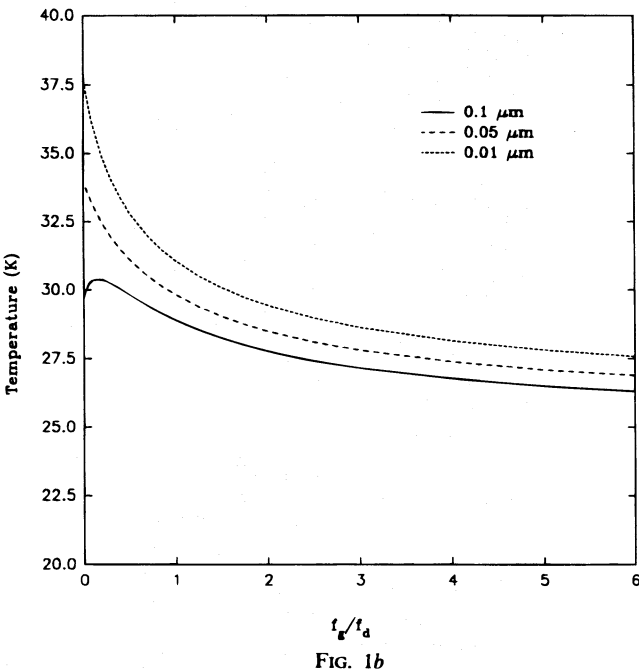
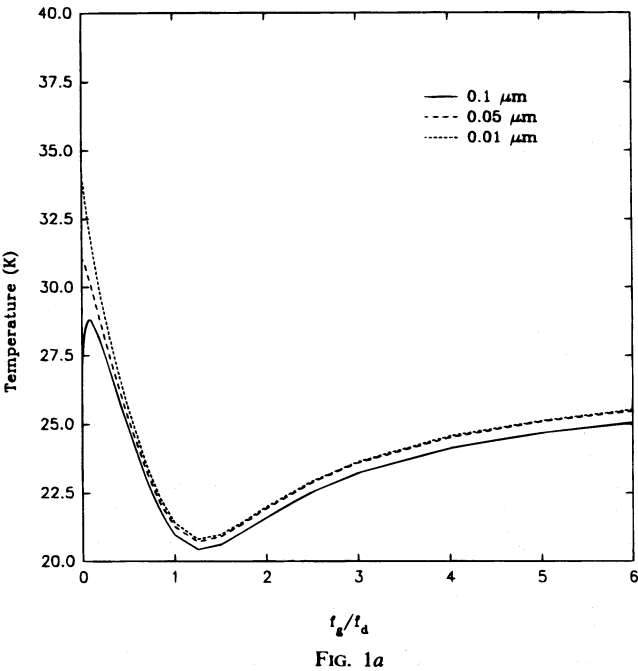


FIG. 1.—Equilibrium dust temperature in the unattenuated ISRF plotted for several grain radii and a variable ratio of graphitic and diamond bonded carbon: (a)  $f_p = 0.4$ , (b)  $f_p = 0.8$ .

## 2. EQUILIBRIUM GRAIN TEMPERATURES IN CARBONS WITH MIXED COMPOSITION

We model the composition of interstellar carbons using a mixture of graphite, diamond, and polyethylene. A void component is also included to simulate the effect of porosity (Pinho & Duley 1994). In some calculations, the graphite component has been replaced by amorphous carbon. An effective medium approximation (EMA) based on the Bruggeman (1935) formalism has been adopted to describe these solids (Smith 1984). The interstellar radiation fields (ISRFs) adopted for these calculations are those of Mathis, Mezger, & Panagia (1983) for the solar neighborhood (when  $A_V = 0$ ) and for a giant molecular cloud (when  $A_V > 0$ ). The formalism used to calculate IR emission by VSGs follows that of Guhathakurta & Draine (1989).

RCN solutions for carbons containing hydrogen,  $sp^2$  carbon, and  $sp^3$  carbon (we ignore any contribution from  $sp^1$  hybridized carbon) are expressed in terms of the atomic

fractions  $x_1$ ,  $x_3$ , and  $x_4$ , respectively, where

$$x_1 + x_3 + x_4 = 1. \tag{1}$$

A fraction,  $f_g$ , of  $sp^2$  carbon is assumed to be in the form of  $C_6$  aromatic rings, while a fraction,  $f_d$ , of  $sp^3$  carbon is assumed to be in the form of six atom diamond-like carbon clusters (Duley 1995). For simplicity, the “aliphatic” component is represented in this mixture by polyethylene. Then the fraction,  $f_p$ , of the aliphatic component is

$$f_p = 1 - f_g - f_d. \tag{2}$$

Figures 1a–1b show equilibrium temperatures versus  $f_g/f_d$  for grains of various radii and  $f_p = 0.4$  and 0.8, respectively, in the unattenuated ISRF ( $A_V = 0$ ). These curves differ from those of Pinho & Duley (1994) due to improvements in the accuracy of our calculations for materials with  $f_g/f_d \leq 1$ . The strong dependence of  $T_d$  on the presence of small amounts of aromatic ring material is evident in these plots and arises

TABLE 1  
AVERAGE EQUILIBRIUM GRAIN TEMPERATURES  $T_d^a$

OBJECT	$f_g/f_d$	$f_p$	$\delta$	$T_d(K)$		
				$A_V = 0$	$A_V = 1$	$A_V = 10$
VI Cyg no. 12 .....	$\infty$	0.4–0.5	0.3–0.7	27	22	12.5
	2	0.4	0.3–0.6	22	17	9.5
	1	0.4–0.6	0.2–0.6	21	16.5	9.0
	0	0.5–0.8	0.2–0.3	32	19	6.5
NGC 7538 IRS 9 .....	0.6	0.05	0.8	21	15–17	9
	0.0	0.3–0.8	0.6–0.7	30–40	17–20	6–7

<sup>a</sup> Calculated for carbonaceous grains whose spectral properties are compatible with observed IR spectra and whose composition and structure satisfy RCN constraints. Note that the ratio  $f_g/f_d$ , the fraction  $f_p$ , and the fraction of carbon  $\delta$  contained in these solids are derived from IR spectra, while  $T_d$  is a predicted quantity.  $T_d$  is not a strong function of grain radius,  $a$ , under these conditions. Values quoted cover radii  $0.01 \leq a \leq 0.1 \mu m$ .

since the inclusion of a small amount of aromatic carbon in a mixture of diamond-like and aliphatic material greatly enhances IR emissivity, while absorption at UV wavelengths is still dominated by these other components.

RCN solutions for diffuse cloud dust (as typified by VI Cyg OB2 no. 12) and dense clouds (as typified by NGC 7538 IRS 9) permit a range of  $f_g/f_d$  and hydrogen content (Duley 1995) and therefore a range of possible equilibrium values for  $T_d$ . Some solutions are given in Table 1 for dust in these objects. The fraction,  $\delta$ , of available carbon, assuming a cosmic carbon abundance of  $3.7 \times 10^{-4}$  relative to hydrogen, contained in this dust is also given in Table 1. Grains are generally found to have  $T_d$  in the range 17–22 K under diffuse cloud conditions ( $A_V \approx 1$ ). This result is not strongly dependent on  $f_g/f_d$  under these conditions, and temperatures are similar to those calculated for pure graphite grains in the same ISRF (Draine & Lee 1984). In all cases, equilibrium grain temperatures are much lower in regions of high  $A_V$  and show no strong dependence on  $f_g/f_d$  or  $f_p$ , although somewhat higher values of  $T_d$  may occur in dust for which  $f_g/f_d$  is large. The presence of voids in these materials has been found to have little influence on  $T_d$  for the RCN solutions given in Table 1.

### 3. NONEQUILIBRIUM IR EMISSION FROM CARBONS WITH MIXED COMPOSITION

Emission spectra of transiently heated VSGs of mixed composition exposed to the ISRF are shown in Figures 2–8. Only particles with radii  $a \lesssim 0.003 \mu\text{m}$  exhibit appreciable excess emission at wavelengths  $\lambda \leq 10 \mu\text{m}$ . Under these conditions, spectra of particles with  $f_p \neq 0$  and small  $f_g$  are all characterized by significant emission at the  $\sim 3.4 \mu\text{m}$  wavelength of the aliphatic  $\text{CH}_n$  stretch. In some cases, this  $3.4 \mu\text{m}$  emission is the dominant spectral feature and is accompanied by additional sharp features at 6.9 and  $13.9 \mu\text{m}$  which can be attributed to other vibrational modes of the polyethylene used to model the aliphatic dust component.  $\text{CH}_n$  absorption is also present in the Allende microdiamond whose optical constants (Lewis, Anders, & Draine 1989) have been used in the present calculation. The strong emission peak at  $3.4\text{--}3.5 \mu\text{m}$  in the lower spectrum of Figure 2 arises as emission from these functional groups and is superimposed on the  $3.4 \mu\text{m}$  polyethylene emission in other spectra. Broad emission bands at  $\sim 5.6$  and  $\sim 8.5 \mu\text{m}$

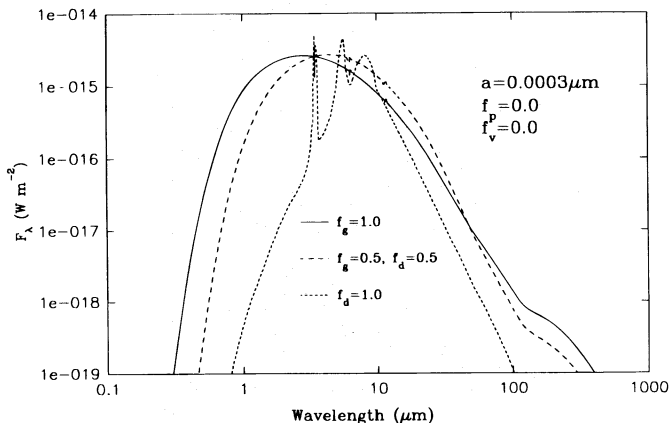


FIG. 2.—IR emission intensity for a  $0.0003 \mu\text{m}$  radius grain subjected to stochastic heating by the ISRF.

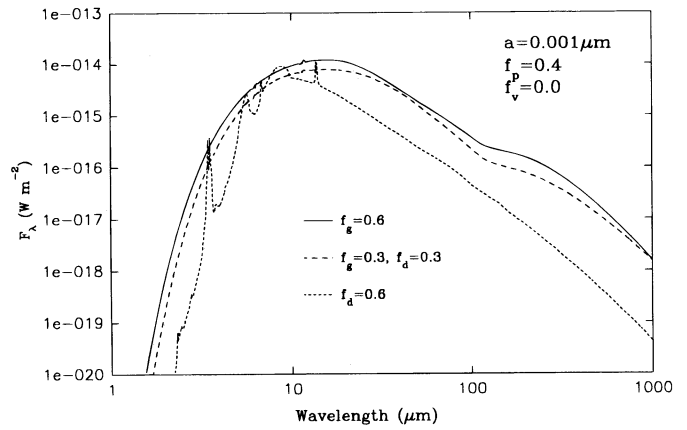


FIG. 3.—Same as Fig. 2, but for  $a = 0.001 \mu\text{m}$  with  $f_p = 0.4, f_v = 0$

are also due to functional groups in the Allende microdiamond material.

Figures 7–8 plot emission spectra for particles with  $a = 0.002 \mu\text{m}$  and show that a sharp peak at  $3.4\text{--}3.5 \mu\text{m}$  is still present, although with much reduced amplitude. Dominant sharp line emission for particles of this size occurs at

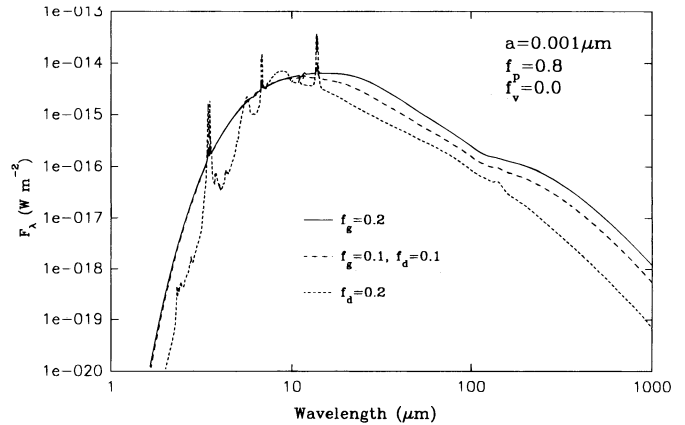


FIG. 4.—Same as Fig. 3, but with  $f_p = 0.8, f_v = 0$

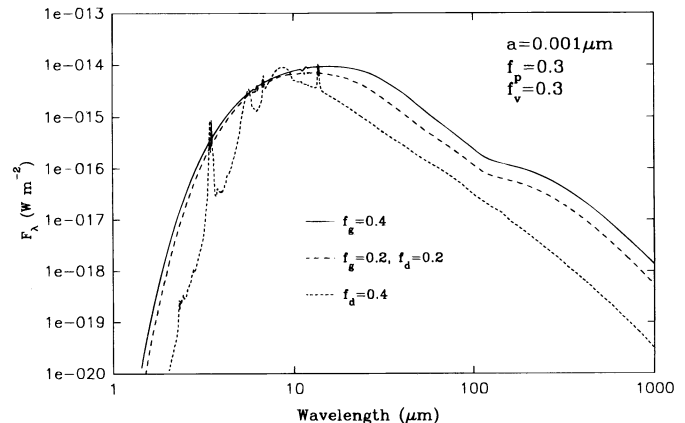


FIG. 5.—Same as Fig. 3, but with  $f_p = 0.3, f_v = 0.3$

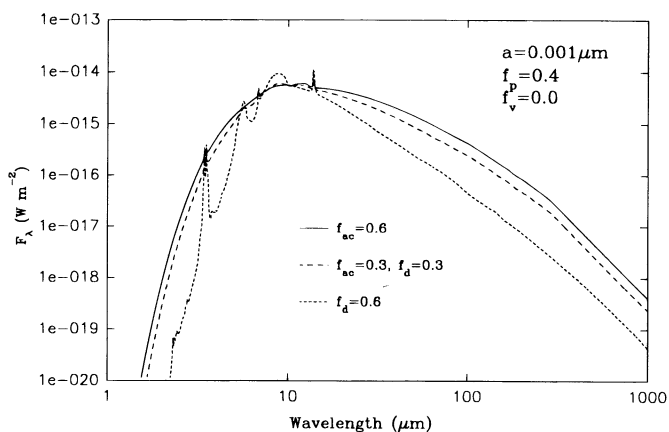


FIG. 6.—Same as Fig. 3, but with graphite replaced with amorphous carbon as the aromatic  $sp^2$  component.

6.9 and 13.9  $\mu\text{m}$ . The presence of porosity has little effect on the emission spectrum under these conditions.

The inclusion of  $sp^2$  aromatic ring material in these mixtures has a significant effect on overall emission and can result in either higher (Fig. 3) or lower (Fig. 7) transient temperatures depending on particle size, composition, and the emission wavelength. The presence of aromatic materials also has the effect of suppressing emission in the  $\text{CH}_n$  bands. Substitution of amorphous carbon for the graphite component in these solids (Fig. 6) has little effect

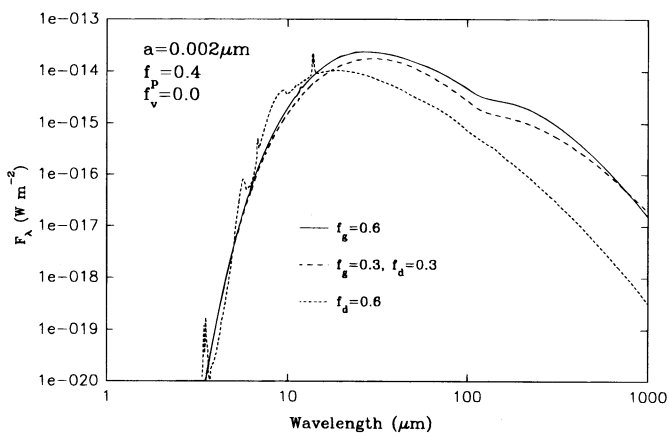


FIG. 7.—Same as Fig. 2, but with  $a = 0.002 \mu\text{m}$ ,  $f_p = 0.4$ ,  $f_v = 0$

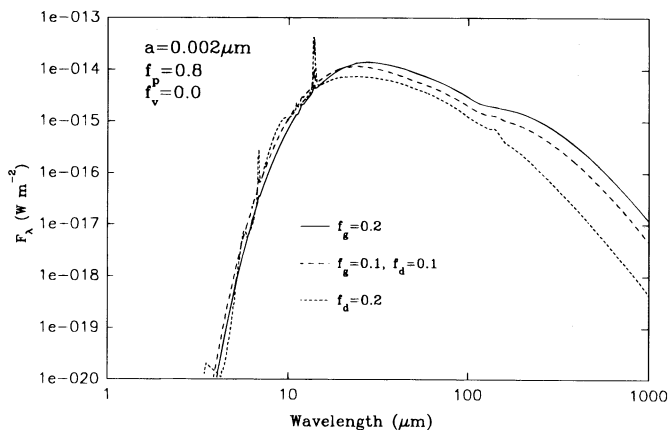


FIG. 8.—Same as Fig. 7, but with  $f_p = 0.8$ ,  $f_v = 0.0$

on emission, except at long wavelengths at which the intensity of emission is slightly reduced.

#### 4. DISCUSSION

The thermal response of carbonaceous grains to the ISRF depends primarily on three factors, all of which are related to grain composition. First, grains must absorb photons from the ISRF. The rate of absorption can be estimated through calculation of the efficiency factor for absorption,  $Q_{\text{abs}}(a, \lambda)$ , which in composite grains is dependent on the optical constants of individual components (e.g., aromatic carbon, diamond, and polymer). As a result, the effective value of  $Q_{\text{abs}}(a, \lambda)$  for a grain of given composition may be quite different than that for any of its components. Thus, grains containing primarily diamond-like carbon may be made to absorb relatively efficiently at visible and near UV wavelengths by the inclusion of  $\lesssim 10\%$  of aromatic carbon.

The second and third factors influencing the thermal response of a composite particle involve the ability to radiate at long wavelengths and the overall heat capacity of the particle. Thermal emissivity depends on the Planck averaged emissivity  $\langle Q_{\text{em}}(a, T_d) \rangle$ , which in turn is determined by the optical constants of the composite particle at IR wavelengths. For materials with a high proportion of wide band gap components such as diamond and polyethylene  $\langle Q_{\text{em}}(a, T_d) \rangle$  can be enhanced greatly by the inclusion of aromatic  $sp^2$  carbon. This effect can be seen in the relative emission for  $f_g = 0.4$  and  $f_d = 0.4$  examples in Figure 5. However, enhanced cooling rates can be offset by increased absorption in the UV, leading to an increase in grain temperature (Fig. 2).

Under all conditions,  $T_d$  is determined by the heat capacity  $C_V$  of the grain and therefore by the heat capacity of its individual components. At high temperatures, this is approximately

$$C_V = 3kN, \quad (3)$$

where  $k$  is the Boltzmann constant and  $N$  is the total number of atoms in the grain. At lower temperatures, heat capacities for individual components  $C_{Vi}$  can be weighted in the same way to obtain an overall  $C_V$  for a composite particle:

$$C_V = \sum_i C_{Vi} x_i. \quad (4)$$

The RCN formalism applied to grain material enables the selection of a subset of solutions that are consistent with observational constraints such as the absorption strength of 3.2–3.5  $\mu\text{m}$   $\text{CH}_n$  transition and the relative amplitudes of individual spectral components. Essentially, this results in sets of  $x_i$  that are internally consistent and which define  $Q_{\text{abs}}(a, \lambda)$ ,  $\langle Q_{\text{em}}(a, T_d) \rangle$  and  $C_V$ . The thermal response of this dust can therefore be calculated in a framework which incorporates observational spectral data in a quantitative manner. As such observational data become available, it may be possible to trace the thermal history of dust from calculations of this kind.

The effect of changing chemical composition on emission by small particles can be seen by comparison of spectra as  $f_g \rightarrow 0$  and  $f_d \rightarrow 0$ . The graphitization of diamond-like carbon particles ( $f_d \rightarrow 0$ ,  $f_g \rightarrow 1$ ) results in an overall increase in IR emission, although spectral changes are different for different sizes of particles. The effect of a transition from



TABLE 2  
THERMAL EMISSION AT 12, 25, 60, AND 100  $\mu\text{m}$  ( $A_V = 0$ ) FROM CARBON DUST WITH MIXED COMPOSITION

RADIUS ( $\mu\text{m}$ )	FRACTION				EMISSION INTENSITY ( $\text{W m}^{-2}$ )				RATIO OF EMISSION			
	$f_g$	$f_d$	$f_p$	$f_v$	12 $\mu\text{m}$	25 $\mu\text{m}$	60 $\mu\text{m}$	100 $\mu\text{m}$	12/25	12/100	25/100	60/100
0.0003.....	1.0	0.0	0.0	0.0	5.80E-16	1.05E-16	5.98E-18	1.38E-18	5.54E+00	4.21E+02	7.59E+01	4.34E+00
	0.5	0.5	0.0	0.0	1.02E-15	1.84E-16	4.72E-18	7.81E-19	5.54E+00	1.31E+03	2.36E+02	6.04E+00
	0.0	1.0	0.0	0.0	4.72E-16	3.35E-17	9.11E-19	1.07E-19	1.41E+01	4.41E+03	3.13E+02	8.51E+00
0.001.....	0.6	0.0	0.4	0.0	1.09E-14	8.88E-15	1.27E-15	3.74E-16	1.23E+00	2.93E+01	2.37E+01	3.40E+00
	0.3	0.3	0.4	0.0	7.24E-15	6.13E-16	9.82E-16	2.24E-16	1.18E+01	3.23E+01	2.74E+00	4.38E+00
	0.0	0.6	0.4	0.0	4.66E-15	1.84E-15	1.69E-16	4.49E-17	2.53E+00	1.04E+02	4.10E+01	3.76E+00
	0.2	0.0	0.8	0.0	6.04E-15	4.88E-15	8.16E-16	2.52E-16	1.24E+00	2.40E+01	1.94E+01	3.24E+00
	0.1	0.1	0.8	0.0	5.21E-15	2.78E-15	4.84E-16	1.58E-16	1.87E+00	3.30E+01	1.76E+01	3.06E+00
	0.0	0.2	0.8	0.0	3.71E-15	1.20E-15	2.65E-16	8.64E-17	3.09E+00	4.29E+01	1.39E+01	3.07E+00
	0.4	0.0	0.3	0.3	8.70E-15	7.38E-15	9.77E-16	2.43E-16	1.18E+00	3.58E+01	3.04E+01	4.02E+00
	0.2	0.2	0.3	0.3	6.94E-15	3.87E-15	4.28E-16	1.19E-16	1.79E+00	5.83E+01	3.25E+01	3.60E+00
	0.0	0.4	0.3	0.3	4.05E-15	9.19E-16	1.18E-16	3.15E-17	4.41E+00	1.29E+02	2.92E+01	3.74E+00
	0.6	0.0	0.4	0.0	5.98E-15	3.63E-15	1.08E-15	4.33E-16	1.65E+00	1.38E+01	8.38E+00	2.49E+00
0.001 <sup>a</sup> .....	0.3	0.3	0.4	0.0	5.55E-15	2.67E-15	6.46E-16	2.48E-16	2.08E+00	2.24E+01	1.08E+01	2.60E+00
	0.0	0.6	0.4	0.0	4.74E-15	1.27E-15	1.71E-16	4.56E-17	3.72E+00	1.04E+02	2.79E+01	3.76E+00
0.002.....	0.6	0.0	0.4	0.0	4.82E-15	2.35E-14	1.22E-14	4.70E-15	2.05E-01	1.03E+00	5.00E+00	2.59E+00
	0.3	0.3	0.4	0.0	3.52E-15	1.64E-14	8.64E-15	2.75E-15	2.15E-01	1.28E+00	5.97E+00	3.14E+00
	0.0	0.6	0.4	0.0	6.23E-15	9.07E-15	2.47E-15	7.24E-16	6.87E-01	8.60E+00	1.25E+01	3.41E+00
	0.2	0.0	0.8	0.0	2.09E-15	1.37E-14	7.19E-15	2.99E-15	1.52E-01	6.99E-01	4.59E+00	2.40E+00
	0.1	0.1	0.8	0.0	2.91E-15	1.17E-14	4.93E-15	1.99E-15	2.50E-01	1.46E+00	5.85E+00	2.48E+00
	0.0	0.2	0.8	0.0	2.42E-15	7.47E-15	3.51E-15	1.22E-15	3.24E-01	1.98E+00	6.12E+00	2.88E+00

NOTES.— $f_g$ ,  $f_d$ ,  $f_p$ , and  $f_v$  are fractional amounts of graphite, diamond, polymer, and void components. Grains are spherical.

<sup>a</sup> Graphite component is replaced with amorphous carbon.

diamond to graphite on emission within the 12, 25, 60, and 100  $\mu\text{m}$  IRAS bands is summarized in Table 2. It is apparent that inclusion of diamond in graphite can enhance the 12/25  $\mu\text{m}$  emission ratio and that the presence of diamond can have a profound effect on 12/100 and 25/100  $\mu\text{m}$  emission ratios.

## 5. CONCLUSIONS

Infrared spectral data indicate that interstellar carbonaceous grains are of mixed composition containing aromatic, aliphatic, and diamond-like carbon components. A model based on the theory of random covalent networks can be used to describe such solids and when combined with an effective medium approximation can be used to calculate grain temperatures and infrared emission. We find that composite carbon grains satisfying RCN constraints

achieve equilibrium grain temperatures that may be as low as 6–7 K in dark clouds. Grain temperatures in diffuse clouds are predicted to be 16–22 K, but they may be as high as 32 K for certain grain compositions when  $A_V = 0$ .

Calculated IR emission from very small composite grains is strongly dependent on both grain size and on composition. Grains with a simulated aliphatic hydrocarbon component can be strong emitters in the 3.4–3.5  $\mu\text{m}$   $\text{CH}_n$  band as well as at wavelengths corresponding to other vibrational modes at higher wavelengths. We find also that inclusion of diamond-like or diamond material in graphitic solids can significantly influence emission at 12  $\mu\text{m}$ .

This work was supported by grants from the NSERC of Canada.

## REFERENCES

- Adamson, A. J., Whittet, D. C. B., & Duley, W. W. 1990, *MNRAS*, 243, 400  
Allamandola, L. J., Sandford, S. A., Tielens, A. G. G. M., & Herbst, T. 1992, *ApJ*, 399, 144  
Angus, J. C., & Hayman, C. C. 1988, *Science*, 241, 913  
Angus, J. C., & Jensen, F. 1988, *J. Vac. Sci. Technol.*, A6, 1778  
Bruggeman, D. A. G. 1935, *Ann. Phys. (Leipzig)*, 24, 636  
Butchart, I., McFadzean, A. D., Whittet, D. C. B., Geballe, T. R., & Greenberg, J. M. 1986, *A&A*, 154, L5  
Draine, B. T., & Lee, H. M. 1984, *ApJ*, 285, 89  
Duley, W. W. 1995, *ApJ*, 445, 240  
Guhathakurta, P., & Draine, B. T. 1989, *ApJ*, 345, 230  
Jones, A. P. 1990, *MNRAS*, 247, 305  
Lewis, R. S., Anders, E., & Draine, B. T. 1989, *Nature*, 339, 117  
Mathis, J. S., Mezger, P. G., & Panagia, N. 1983, *A&A*, 128, 212  
Pendleton, Y. J., Sandford, S. A., Allamandola, L. J., Tielens, A. G. G. M., & Sellgren, K. 1994, *ApJ*, 437, 683  
Pinho, G. P., & Duley, W. W. 1994, *MNRAS*, 269, 121  
Sandford, S. A., Allamandola, L. J., Tielens, A. G. G. M., Sellgren, K., Tapia, M., & Pendleton, Y. 1991, *ApJ*, 371, 607  
Sellgren, K., Smith, R. G., & Brooke, T. Y. 1994, *ApJ*, 433, 179  
Smith, F. W. 1984, *J. Appl. Phys.*, 55, 764  
Tamor, M. A., Vassell, W. C., & Carduner, K. R. 1991, *Appl. Phys. Lett.*, 58, 692  
Tamor, M. A., & Wu, C. H. 1990, *J. Appl. Phys.*, 67, 1007  
Wickramasinghe, D. T., & Allen, D. A. 1980, *Nature*, 287, 518